

A direct connection between quantum Hall plateaus and exact pair states in a 2D electron gas

Research Article

Wenhua Hai^{1*}, Zejun Li¹, Kewen Xiao¹

¹ Department of physics and Key Laboratory of Low-dimensional Quantum Structures and Quantum Control of Ministry of Education, Hunan Normal University, Changsha 410081, China

Received 25 June 2011; accepted 25 July 2011

Abstract: It is previously found that the two-dimensional (2D) electron-pair in a homogeneous magnetic field has a set of exact solutions for a denumerably infinite set of magnetic fields. Here we demonstrate that as a function of magnetic field a band-like structure of energy associated with the exact pair states exists. A direct and simple connection between the pair states and the quantum Hall effect is revealed by the band-like structure of the hydrogen "pseudo-atom". From such a connection one can predict the sites and widths of the integral and fractional quantum Hall plateaus for an electron gas in a GaAs-Al_xGa_{1-x}As heterojunction. The results are in good agreement with the existing experimental data.

PACS (2008): 73.43.Cd; 73.43.-f; 05.30.Fk; 03.65.Ge; 73.20.-r

Keywords: quantum Hall effect • hydrogen pseudo-atom • band-like structure • exact pair state • 2D electron gas
© Versita Sp. z o.o.

1. Introduction

The integral and fractional quantum Hall effect (QHE) appeared in a single experiment [1–3] as a single phenomenon. However, in the previous works [4–25] the single phenomenon was explained by using several different theories. The integral QHE was explained as a property of uncorrelated electrons by adopting a single-electron model in the presence of a magnetic field. Differing from this, the fractional QHE was regarded as a manifestation of a quantum fluid consisting of strongly correlated electrons interacting with a strong magnetic field. Even some of the fractional quantum Hall plateaus were resided in

the integral QHE of composite particles and the others were associated with the fractional QHE of the composite particles [3, 21, 22]. Particularly, some of the theories can predict the sites of the Hall plateaus only, but cannot calculate the widths of the plateaus.

All of the experiments and theories are based on the same fundamental system: a two-dimensional (2D) electronic gas in a homogeneous magnetic field. An important experimental fact is that the quantum Hall plateaus are associated with the minima of the diagonal-resistance and the lowest minima vanish approximately, which correspond to a discrete set of magnetic fields [1–3, 21]. Seeking a single theory to comprehensively describe the integral and fractional QHEs is an interesting work. However, this is hard when the higher minima are taken into account.

It should be noticed that a single 2D electron in a homogeneous magnetic field can be described by the Schrödinger

*E-mail: whhai2005@yahoo.com.cn

equation of a 2D harmonic oscillator $[-\frac{\hbar^2}{2\mu}(\partial^2/\partial x^2 + \partial^2/\partial y^2) + \frac{1}{2}\mu\omega^2 r^2 + \omega l_z]\psi = E\psi$, with positive energy E . Under the transformation to parabolic coordinate $x' = (x^2 - y^2)/2$, $y' = xy$, $r' = \sqrt{x'^2 + y'^2} = \frac{1}{2}(x^2 + y^2) = \frac{1}{2}r^2$, this equation becomes the equivalent hydrogen atom's model $[-\frac{\hbar^2}{2\mu}(\partial^2/\partial x'^2 + \partial^2/\partial y'^2) - e'^2/r']\psi = E'\psi$ with the effective "electron charge" $e' = -\sqrt{(E - \omega l_z)/2}$ and negative "energy" $E' = -\frac{1}{2}\mu\omega^2$. When two electrons are considered, a repulsive electron-electron interaction potential of the form $e^2/(2r')^{3/2}$ is added into the equivalent hydrogen equation. The equivalent hydrogen atom's model is valid only for the 2D case. It is important to note that such a dimensionality exists in the quantum Hall systems. We also notice that a 2D electron-pair in a homogeneous magnetic field has a set of exact solutions for a denumerably infinite set of magnetic field [26–31], which represents stable stationary states of the system. On the other hand, the relations between Hall effects and analytical solutions of some quantum systems have been investigated recently [32, 33]. It is well known that extension from the exact solutions of a hydrogen atom to the shell structures of multi-electron atoms is natural, since the exact solutions indicate the stable stationary states to be occupied by the multiple electrons. The relation between the exact solutions of a hydrogen atom and the atomic shell structures hints us a connection between the exact solutions of the 2D electron-pair and the quantum Hall structures.

Differing from the single-electron model [5], for a 2D magnetically trapped electron-pair both the Coulomb and harmonic potentials work simultaneously and the exact solutions of the system depend on some particular values of the harmonic oscillator frequency determined by the magnetic field intensity [26–31]. In this paper we apply the exact results to a 2D magnetically trapped electronic gas and seek its level structure that consists of the degenerate lowest Landau level of center-of-mass motion and the non-degenerate energy band-likes of relative motion based on the electron-pairs. Any discrete exact level indicates the center site of the corresponding energy band-like and therefore means higher stability of the electron-pairs in the exact states. Unlike the famous theory based on many-body wave functions [8, 9], our method demonstrates a direct and simple connection between the pair states and the integral and fractional QHEs comprehensively, through the band-like structure of the hydrogen "pseudo-atom". The results suggest an alternative method which enables us to predict the sites of the Hall plateaus and to estimate the plateau widths directly in a good agreement with the known experimental data.

2. Exact pair states and approximate band-like structure

Quantum motion of a 2D electron-pair in a homogeneous magnetic field toward z direction is dominated by the stationary-state Schrödinger equation [26–28, 30, 34],

$$\sum_{i=1}^2 \left[-\frac{\hbar^2}{2m_{eff}} \nabla_i^2 + \frac{1}{2}m_{eff}\omega^2(x_i^2 + y_i^2) + \omega l_i + \frac{e^2}{\epsilon r} \right] \Psi = E_T \Psi, \quad (1)$$

where E_T is the total energy, m_{eff} and $-e$ are the effective mass and charge [5, 34] of a single electron, x_i, y_i and ∇_i^2 are the coordinates and Laplace operator of i th electron, $r = \sqrt{(x_2 - x_1)^2 + (y_2 - y_1)^2}$ is the relative radial coordinate, $l_i = x_i p_{y_i} - y_i p_{x_i}$ denotes the z -component angular momentum of i th electron, $\omega = eB/(2cm_{eff})$ represents the Larmor cyclotron frequency with the light velocity c and magnetic field B , and ϵ is the effective dielectric constant of the background semiconductor [21, 34]. We set $E_T = E^{(c)} + E$ and $\Psi = \psi^{(c)}(\mathbf{R})\psi(\mathbf{r})$, where $E^{(c)}$ and E denote the center-of-mass and relative energies, $\psi^{(c)}$ and ψ are the center-of-mass and relative wave-functions, and \mathbf{R} and \mathbf{r} are the center-of-mass and relative coordinate vectors, $\mathbf{r} = \mathbf{r}_2 - \mathbf{r}_1 = (x_2 - x_1)\mathbf{e}_x + (y_2 - y_1)\mathbf{e}_y = x\mathbf{e}_x + y\mathbf{e}_y$, $\mathbf{R} = (\mathbf{r}_1 + \mathbf{r}_2)/2 = (x_2 + x_1)\mathbf{e}_x/2 + (y_2 + y_1)\mathbf{e}_y/2 = X\mathbf{e}_x + Y\mathbf{e}_y$ with \mathbf{e}_x and \mathbf{e}_y being the unit vectors in x and y directions. In the new coordinate systems, Eq. (1) is separated to the center-of-mass and relative motion equations

$$\begin{cases} \left[-\frac{\hbar^2}{2M} \nabla_R^2 + \frac{1}{2}M\omega^2 R^2 + \omega L_z \right] \psi^{(c)} = E^{(c)} \psi^{(c)}, \\ \left[-\frac{\hbar^2}{2\mu} \nabla_r^2 + \frac{1}{2}\mu\omega^2 r^2 + \omega l_z + \frac{e^2}{\epsilon r} \right] \psi = E \psi, \end{cases} \quad (2)$$

where $\mu = m_{eff}/2$ is the reduced mass, $M = 2m_{eff}$ denotes the total mass, $L_z = XP_y - YP_x$ and $l_z = xp_y - yp_x$ are the z -component angular momenta on the center-of-mass and relative coordinate frames respectively. Noticing the Pauli's exclusion principle and the condensed states of the electron gas observed in the quantum Hall effect, we use the simplification in which the two paired electrons are in the opposite spin orientations with zero total spin and the spin triplet states with nonzero total spin are not considered. Such a simplification helps us to treat the many-electron system in a high magnetic field as a many-boson system with the electron pairs occupying the lowest-energy states, which has been adopted in the more elaborate many-electron theory [8, 9]. Moreover, in the considered strong-field case, the spin-orbit couple could be negligible [35], so no spin term appears in Eqs. (1) and (2).

It was early found that the electron of two-body (atom) hydrogen experiences an attractive Coulomb force and its quantum-mechanical exact solutions are associated with the shell structures of multi-electron atoms [35]. Similarly, for a sufficiently strong magnetic field B and relatively large distance r any electron governed by the second of Eq. (2) experiences an attractive combined force of the attractive harmonic force and repulsive Coulomb force. Under the parabolic coordinate $x' = (x^2 - y^2)/2$, $y' = xy$, the second of Eq. (2) becomes an equivalent hydrogen atom's model with electron-electron interaction $\frac{e^2}{\epsilon(2r')^{3/2}}$, so the corresponding energy-shell structure is expectable. Therefore, we can regard the 2D magnetically trapped electron gas as a multi-electron "pseudo-atom", and establish a similar connection between the exact solutions of the electron-pair and the quantum Hall structure of the multiple electrons, in which the discrete magnetic field fitting the exact solutions correspond to the center sites of the Hall plateaus. Physically, such a "pseudo-atom" has higher stability when more electron-pairs occupy the lowest levels determined by Eq. (2).

The center-of-mass motion obeys the same equation as a single charged particle with mass $M = 2m_{eff}$ and charge $q = -2e$ in a homogeneous magnetic field, which has the well-known solution [30, 35, 36]

$$\psi_{n_c m_c}^{(c)} = e^{im_c \phi_c - R^2/2} R^{|m_c|} F(-n_c, |m_c| + 1, R^2) \quad (3)$$

for the center-of-mass energies (Landau levels) $E^{(c)}/(\hbar\omega) = E_{n_c m_c}^{(c)}/(\hbar\omega) = 2n_c + |m_c| + m_c + 1 = 1, 2, 3, \dots$. Here $n_c = 0, 1, 2, \dots$; $m_c = 0, \pm 1, \pm 2, \dots$; $F(-n_c, |m_c| + 1, R^2)$ denotes the confluent hypergeometric function and ϕ_c is the center-of-mass angular coordinate. The radial coordinate R has been normalized by the magnetic length $a_c = \sqrt{\hbar/(M\omega)}$. Obviously, $\psi_{n_c m_c}^{(c)}$ expresses the multiple degenerate states, since the energy $E_{n_c, -|m_c|}^{(c)}/(\hbar\omega) = 2n_c + 1$ corresponds to the $M_{n_c} + 1$ states with $|m_c| + m_c = 0$ for $m_c = 0, -1, -2, \dots, -M_{n_c}$ and any ω . The largest magnetic quantum number M_{n_c} and principal quantum number n_c are limited by the mean square-radius (or area) $\overline{R_{n_c m_c}^2} = \langle \psi_{n_c m_c}^{(c)} | R^2 | \psi_{n_c m_c}^{(c)} \rangle / \langle \psi_{n_c m_c}^{(c)} | \psi_{n_c m_c}^{(c)} \rangle \leq R_0^2$ for a 2D circular sample with radius R_0 . Taking the lowest Landau level ($n_c = 0$) $E_{0, -|m_c|}^{(c)} = 1(\hbar\omega)$ as an example, this equation gives $\overline{R_{0, m_c}^2} = (|m_c| + 1)(a_c^2) \leq R_0^2$. Thus we have the degeneracy of the lowest Landau level

$$\begin{aligned} M_0 + 1 &= \max\{|m_c|\} + 1 = R_0^2/a_c^2 = 2\pi R_0^2 M\omega/\hbar \\ &= 2\pi R_0^2 eB/(\hbar c) = \Phi/\Phi_0, \end{aligned} \quad (4)$$

where $\Phi_0 = hc/(2e)$ is the magnetic flux quantum of the electron-pairs and $\Phi = \pi R_0^2 B$ denotes the magnetic flux through the sample, which equates $(M_0 + 1)$ times the Φ_0 .

We are interested in the exact solutions of the relative motion equation and the corresponding properties of the particle-pairs, including the application to the integral and fractional QHE. Adopting the relative angular coordinate ϕ and normalized polar coordinate $\rho = r/a_r$ with $a_r = \sqrt{2\hbar/(m_{eff}\omega)} = 2a_c$, the exact relative wave function can be written in the form [26–28, 30]

$$\psi(\rho, \phi) = A e^{im\phi - \rho^2/2} \rho^{|m|} u(\rho), \quad m = 0, \pm 1, \dots \quad (5)$$

with the normalization constant A and undetermined function $u(\rho)$. Applying Eq. (5) to Eq. (2) we arrive at the 1D dimensionless equation

$$\begin{aligned} \frac{d^2 u}{d\rho^2} + \left(\frac{2|m| + 1}{\rho} - 2\rho \right) \frac{du}{d\rho} \\ + \left[2 \left(\frac{E'}{\hbar\omega} - |m| - 1 \right) - \frac{\sigma}{\rho} \right] u = 0, \quad (6) \\ \sigma = \sqrt{2 \frac{e^4 m_{eff}}{\hbar^3 \omega \epsilon^2}} = \sqrt{\frac{e^2/(\epsilon a_0)}{\hbar\omega/2}}. \end{aligned}$$

Here E' is equal to $E - m\hbar\omega$ and the dimensionless constant σ^2 expresses the importance of the Coulomb potential $e^2/(\epsilon a_0)$ compared to the harmonic level $\hbar\omega$, where $a_0 = \epsilon\hbar^2/(m_{eff}e^2)$ is the effective Bohr radius. According to the form of the equation for u we expect the power-series solution [30] $u = \sum_{i=0}^n C_i \rho^i$ for $n = 1, 2, \dots$ and $C_i = \text{constant}$. Inserting the series into Eq. (6) yields the algebraic equation

$$\begin{aligned} \sum_{i=0}^n \{ (i^2 + 2i|m|)\rho^{i-2} + \sigma\rho^{i-1} \\ + 2[E'/(\hbar\omega) - |m| - 1 - i]\rho^i \} C_i = 0. \quad (7) \end{aligned}$$

This equation can be satisfied if and only if the constants C_i , σ and E obey the algebraic equations of three-term recurrence [30]

$$\begin{aligned} E'/(\hbar\omega) &= n + |m| + 1, \\ (n-j)(n-j+2|m|)C_{n-j} - \sigma C_{n-j-1} \\ &+ 2(j+2)C_{n-j-2} = 0 \end{aligned} \quad (8)$$

for $C_0 = 1$, $C_{-1} = C_{n+1} = 0$, $j = -1, 0, 1, \dots, (n-1)$. By using a computer we have solved the algebraic equations from Eq. (8) for $n = 1, 2, \dots, 30$; $|m| = 0, 1, \dots, 30$. Several simple solutions are listed as the following:

$$\begin{aligned} n = 1, \quad \sigma^2 &= (\sigma_{1|m|}^{(1)})^2 = 2(2|m| + 1), \quad C_1 = \frac{\sigma_{1|m|}^{(1)}}{2|m|+1}; \\ n = 2, \quad (\sigma_{2|m|}^{(1)})^2 &= 4(4|m| + 3), \quad C_1 = \frac{\sigma_{2|m|}^{(1)}}{2|m|+1} = \frac{\sigma_{2|m|}^{(1)}}{2} C_2; \\ n = 3, \quad (\sigma_{3|m|}^{(1)})^2 &= 20(|m| + 1) \pm 2\sqrt{64m^2 + 128|m| + 73}; \\ n = 4, \quad (\sigma_{4|m|}^{(1)})^2 &= 50 + 40|m| \pm 6\sqrt{16m^2 + 40|m| + 33}. \end{aligned} \quad (9)$$

Here we have set $l = 1, 2, \dots, l_{max}$, $l_{max} = n$ for even n and $l_{max} = (n + 1)$ for odd n , which is the label of the different solutions of $\sigma_{n|m|}$ for a set of fixed quantum numbers n and $|m|$. For the repulsive Coulomb potential the $\sigma_{n|m|}$ takes positive values which are arranged in order of $l = 1, 2, \dots, l_{max}/2$ such that $\sigma_{n|m|}^{(1)}$ denotes the smallest one of $\sigma_{n|m|}^{(l)}$. In the cases $n = 3, 4$, any C_i is a complicated function of $|m|$, which is not shown in Eq. (9). For $n \geq 5$ the computer cannot give C_i and σ as the explicit functions of $|m|$, however, we can numerically calculate them from Eq. (8) for any given n and $|m|$. Noticing the above-mentioned relationships between ω and σ , and between B and ω , the quantized σ values imply the quantization of the cyclotron frequency ω , magnetic intensity B and energy E ,

$$\begin{aligned}\omega &= \omega_{n|m|}^{(l)} = \frac{\omega_0}{(\sigma_{n|m|}^{(l)})^2}, & \omega_0 &= \frac{2e^4 m_{eff}}{\hbar^3 \epsilon^2}, \\ B &= B_{n|m|}^{(l)} = \frac{B_0}{(\sigma_{n|m|}^{(l)})^2}, & B_0 &= \frac{4e^3 m_{eff}^2 c}{\hbar^3 \epsilon^2}, \\ E &= E_{nm}^{(l)} = E'_{n|m|} + m\hbar\omega_{n|m|}^{(l)} \\ &= (n + |m| + m + 1)\hbar\omega_{n|m|}^{(l)} \\ &= \frac{(n + |m| + m + 1)}{(\sigma_{n|m|}^{(l)})^2} \hbar\omega_0.\end{aligned}\quad (10)$$

The constant $B_0 = 2cm_{eff}\omega_0/e$ depends on the sample material and can be determined by experiments. The dependence of C_i and $\rho(a_r)$ on the quantum numbers $n, |m|, l$ leads to the relative wavefunction $\psi = \psi_{nm}^{(l)}$ of the equivalent 2D hydrogen atom.

Given Eqs. (9), (10) and wavefunctions $\psi = \psi_{nm}^{(l)}$, we find the following interesting properties:

a) In Eq. (5) the series solution $u = \sum_{i=0}^n C_i \rho^i$ can be truncated at quantum number n iff the magnetic strength is quantized, as in Eq. (10). This truncation condition gives a denumerably infinite set $\{B_{n|m|}^{(l)}\}$ of the magnetic field values. The corresponding denumerably infinite sets of frequencies and eigenenergies read $\{\omega_{n|m|}^{(l)}\}$ and $\{E_{nm}^{(l)}\}$. In the case of a stationary harmonic oscillator we have known that the wavefunctions must be in the series form of Hermitian polynomial and there exist a denumerably infinite set $\{\psi_n, E_n\}$ of wavefunctions and eigenenergies for a fixed frequency value. However, based on the relative equation of Eq. (2) we analytically and numerically find that for any fixed frequency $\omega \in \{\omega_{n|m|}^{(l)}\}$ the eigenenergies and wavefunctions are determined to only the two pairs $(E_{n|m|}^{(l)}, \psi_{n|m|}^{(l)})$ and $(E_{n,-|m|}^{(l)}, \psi_{n,-|m|}^{(l)})$, since the frequency is related to $|m|$ but the energy and wavefunction are related to m . Therefore, after treating the relative states as the internal states of the system, the

electron-pair under the magnetic field $B \in \{B_{n|m|}^{(l)}\}$ being a two-internal-level system with two non-degenerate relative states, the paramagnetic state ($m > 0$) and diamagnetic state ($m < 0$). The diamagnetic state is the ground state with $(|m| + m = 0)$ and the paramagnetic state is the excited state with $(|m| + m = 2|m|)$. The level difference between the two states reads $2m\hbar\omega_{n|m|}^{(l)}$. Because the amplitude $|\psi_{nm}^{(l)}|$ depends on $|m|$ rather than m so the paramagnetic and diamagnetic states have the same relative probability distribution.

b) The size of the electron-pair in the states $\psi_{nm}^{(l)}$ of lower quantum numbers is in the order of the relative magnetic length $a_r = a_{n|m|}^{(l)} = \sqrt{2\hbar/(m_{eff}\omega_{n|m|}^{(l)})}$, which may approach the size of the hydrogen atom in lower excited state, when the magnetic field is strong enough. For example, the magnetic field value $B \sim 30$ Tesla (T) corresponds to the cyclotron frequency $\omega \sim 10^{13}$ Hz and magnetic length $a_r \sim 10^{-9}$ m, and in the simplest state $\psi_{1,0}^{(1)} = Ae^{-\rho^2/2}(1 + C_1\rho) = Ae^{-\rho^2/2}(1 + \sqrt{2}\rho)$, we have the mean radius $\bar{r}_{1,0}^{(1)} = \langle \psi_{1,0}^{(1)} | r | \psi_{1,0}^{(1)} \rangle / \langle \psi_{1,0}^{(1)} | \psi_{1,0}^{(1)} \rangle = 1.15739(a_{1,0}^{(1)}) \sim 10^{-9}$ m.

c) There are two kinds of quantum transitions between the internal states $\psi_{nm}^{(l)}$ for the electron-pair. One is the transitions between the ground and excited states of the relative motion determined by a fixed magnetic field $B_{n|m|}^{(l)}$, which can be operated by using a laser with the frequency $\omega_L = 2|m|\omega_{n|m|}^{(l)}$. Because the amplitude $|\psi_{nm}^{(l)}|$ only depends on $|m|$, the transition between m state and $-m$ state does not change the relative probability density of the particle-pair, but varies the direction of angular momentum. Another kind of transitions occurs between the internal states with different magnetic field. Therefore, this kind of transitions can be controlled by adjusting the magnetic field from one value of $\{B_{n|m|}^{(l)}\}$ to another value. These quantum transitions are probably applicable for performing the quantum logic operations.

d) The positive parameter $\sigma_{n|m|}^{(l)}$ has a minimal value $\sigma_{1,0}^{(1)} = \sqrt{2}$ as in Eq. (9), which corresponds to the upper critical magnetic field and lower critical magnetic length across which the finite series solution $\psi_{nm}^{(l)}$ is no longer valid. For a pure electron-pair Eqs. (9) and (10) give the largest magnetic intensity $B_{1,0}^{(1)} = B_0/2 = 2m_{eff}^2 e^3 c / (\epsilon^2 \hbar^3) = 2m_e^2 e^3 c / \hbar^3 \approx 4.7 \times 10^5$ T with m_e being the rest mass of a free electron, which cannot be experimentally realized yet. Noticing the experimentally allowable magnetic intensity $B < 10^2$ T, the truncation condition (10) requires the parameter $(\sigma_{nm}^{(l)})^2$ being greater than 10^3 which is related to very large quantum numbers n and m . However, if one adopts the modulation-doped GaAs-Al_xGa_{1-x}As heterojunction and let the 2D electrons exist in GaAs at the interface between GaAs and Al_xGa_{1-x}As [5, 8, 9, 34], the corresponding effective mass and dielectric constant become [34] $m_{eff} = 0.067m_e$, $\epsilon \approx 13$ such that Eq. (10)

gives the largest magnetic field value $B_{1,0}^{(1)} \approx 12.4842$ T, such a magnetic field is experimentally realizable. The largest magnetic field value $B_{1,0}^{(1)}$ determines the lowest critical magnetic length $a_{1|0}^{(1)}$. By improving the quality of the GaAs-Al_xGa_{1-x}As interface, the effective mass m_{eff} and dielectric constant ϵ can be adjusted in the wide regions (in general, $m_{eff} \geq 0.065m_e$ and $\epsilon \geq 1$) in a practical experiment [37, 38], therefore, we can obtain the upper critical magnetic field in a large region. For instance, in Fig. 1 of reference [1] the largest magnetic field of a Hall plateau is $B_{1,0}^{(1)} = 15$ T which is associated with the parameters obeying $m_{eff}/\epsilon \approx 0.0056m_e$. Such a parameter region contains $m_{eff} = 0.067m_e$, $\epsilon \approx 11.9$ and $\epsilon \approx 13$, $m_{eff} = 0.073m_e$. However, we cannot estimate the values of m_{eff} and ϵ from reference [3], since we cannot find the largest magnetic field of a plateau from this paper.

The necessary and sufficient conditions for the truncation in Eq. (10) infer that there have only the series solutions with infinite terms for the magnetic field outside the denumerably infinite set $\{B_{n|m}^{(l)}\}$, namely the infinite series solutions exist for the continuous set $B \in (B_{n|m}^{(l)}, B_{n'|m'}^{(l')})$ of magnetic field, in which the states and energies cannot be included by $\{\psi_{nm}^{(l)}\}$ and $\{E_{nm}^{(l)}\}$, where $B_{n|m}^{(l)}$ and $B_{n'|m'}^{(l')}$ are two adjacent points of the set $\{B_{n|m}^{(l)}\}$. Although the infinite series solutions may be convergent, the discrete quantum levels $\{E_{nm}^{(l)}\}$ and quantum states $\{\psi_{nm}^{(l)}\}$ of the equivalent hydrogen atom are particularly meaningful, since for a strong magnetic field $B_{n|m}^{(l)}$ the interval $\Delta B_{n|m}^{(l)} = B_{n'|m'}^{(l')} - B_{n|m}^{(l)}$ is much less than any one of the $B_{n|m}^{(l)}$ and $B_{n'|m'}^{(l')}$ that makes the quantum perturbation theory applicable [26–28]. When the magnetic field is around the point $B_{n|m}^{(l)}$, the corresponding frequency ω approaches $\omega_{n|m}^{(l)}$ and the frequency difference obeys

$$\begin{aligned} |\delta\omega_{n|m}^{(l)}| &= |\omega - \omega_{n|m}^{(l)}| \\ < \Delta\omega_{n|m}^{(l)} &= \omega_{n'|m'}^{(l')} - \omega_{n|m}^{(l)} \ll \omega_{n|m}^{(l)}. \end{aligned} \quad (11)$$

Hence the second and third terms of the relative motion equation in Eq. (2) can be expand as $\frac{1}{2}\mu\omega^2r^2 + \omega l_z = \frac{1}{2}\mu(\omega_{n|m}^{(l)} + \delta\omega_{n|m}^{(l)})^2r^2 + (\omega_{n|m}^{(l)} + \delta\omega_{n|m}^{(l)})l_z \approx \frac{1}{2}\mu(\omega_{n|m}^{(l)})^2r^2 + \omega_{n|m}^{(l)}l_z + \delta\omega_{n|m}^{(l)}(\mu\omega_{n|m}^{(l)}r^2 + l_z)$. Then we can treat the weak terms proportional to $\delta\omega_{n|m}^{(l)}$ as the perturbation potential

$$H'_{n|m}{}^{(l)}(r) = \delta\omega_{n|m}^{(l)}(\mu\omega_{n|m}^{(l)}r^2 + l_z) \quad (12)$$

and obtain the corrections to the state $\psi_{nm}^{(l)}$ and energy $E_{nm}^{(l)}$ from the normal quantum perturbation theory [35]. For instance, from Eqs. (8), (9) and (10) we have the two

neighboring points of the set $\{B_{n|m}^{(l)}\}$ as $B_{1,1}^{(1)} = B_0/6$ and $B_{11,0}^{(1)} = 0.1717B_0$ with $(\sigma_{1,1}^{(1)} = \sqrt{6}, \omega_{1,1}^{(1)} = \omega_0/6, E_{1,-1}^{(1)} = \hbar\omega_0/3)$ and $(\sigma_{11,0}^{(1)} = 2.4139, \omega_{11,0}^{(1)} = 0.1717\omega_0, E_{11,0}^{(1)} = 2.0593\hbar\omega_0)$ respectively. The states and energies corresponding to the magnetic field in the small regions $B \in (B_{1,1}^{(1)}, B_{11,0}^{(1)})$ with width $\Delta B_{1,1}^{(1)} = B_{11,0}^{(1)} - B_{1,1}^{(1)} = 0.005B_0$ cannot be included by $\psi_{nm}^{(l)}$ and $E_{nm}^{(l)}$. Because $\Delta B_{1,1}^{(1)}$ is much less than $B_{1,1}^{(1)}$ and $E_{1,-1}^{(1)}$ is less than $E_{1,1}^{(1)}$ and $E_{11,0}^{(1)}$, and the state $\psi_{1,-1}^{(1)}$ is fixed at $B = B_{1,1}^{(1)}$, we can use the quantum perturbation theory to construct the perturbed solution.

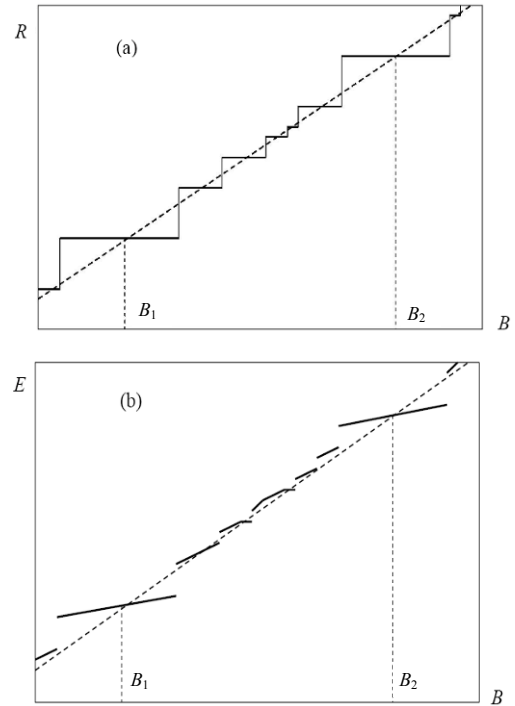


Figure 1. Schematic diagrams for the correspondence between (a) the Hall resistance R and (b) the relative energy E . Two wide Hall plateaus are indicated by the magnetic strengths B_1, B_2 between which the Hall plateaus may be experimentally unmeasurable narrow. The quantities plotted in the figure are in arbitrary units.

We assume that the denumerably infinite set $\{B_{n|m}^{(l)}\}$ corresponds to center positions of infinite Hall plateaus which contains many unmeasurable narrow plateaus [5], as indicated in the schematic diagram of Fig. 1a. Given $\psi_{1,-1}^{(1)}$ and $H'_{n|m}{}^{(l)}(r)$ of Eq. (12), the first-order perturbed solution to the state $\psi_{1,-1}^{(1)}$ in the field region of the plateau centered at $B_{1,1}^{(1)}$ can be easily constructed. The corresponding

energy correction to $E_{1,-1}^{(1)}$ reads

$$\delta E_{1,-1}^{(1)} = \delta \omega_{1,-1}^{(1)} \frac{\langle \psi_{1,-1}^{(1)} | (\mu \omega_{1,-1}^{(1)} r^2 + l_z) | \psi_{1,-1}^{(1)} \rangle}{\langle \psi_{1,-1}^{(1)} | \psi_{1,-1}^{(1)} \rangle} \quad (13)$$

with $|\delta \omega_{1,-1}^{(1)}| = |\omega - \omega_{1,-1}^{(1)}| < \Delta \omega_{1,-1} = \omega_{1,0}^{(1)} - \omega_{1,-1}^{(1)} = 0.005\omega_0$. From Eqs. (5) and (9) we obtain $\psi_{1,-1}^{(1)} = Ae^{i\phi - \rho^2/2} \rho(1 + \sqrt{6}\rho/3)$. The application of this function to Eq. (13) results in $|\delta E_{1,-1}^{(1)}| = \hbar |\delta \omega_{1,-1}^{(1)}| < 0.005\hbar\omega_0$. The corresponding total energy becomes $E = E_{1,-1}^{(1)} + \delta E_{1,-1}^{(1)}$. Noticing $|\delta \omega_{n|m}^{(1)}| \ll \omega_{n|m}^{(1)}$, $\langle \psi_{nm}^{(1)} | r^2 | \psi_{nm}^{(1)} \rangle > 0$, and $l_z \psi_{nm}^{(1)} = m \psi_{nm}^{(1)}$, we can obtain the eigenenergies $E = E_{nm}^{(l)} + \delta E_{nm}^{(l)}$ with $|\delta E_{nm}^{(l)}| \ll E_{nm}^{(l)}$ for any field region of the plateau centered at $B_{n|m}^{(l)}$. The continuous changes of magnetic field in such a region lead to a energy band-like of width $\max\{\delta E_{nm}^{(l)}\}$ and energy gap-like with width $(\max\{\Delta E_{nm}^{(l)}\} - \max\{\delta E_{nm}^{(l)}\}) \geq 0$, where $\max\{\delta E_{nm}^{(l)}\}$ denotes the maximal value of $\delta E_{nm}^{(l)}$ and $\Delta E_{nm}^{(l)} = |E_{n',m'}^{(l)} - E_{nm}^{(l)}|$, as shown in Fig. 1b. Clearly, as a function of magnetic field Fig. 1b displays a band-like structure of energy. Therefore, the discrete levels $\{E_{n,-|m}^{(l)}\}$ indicate the center sites of the corresponding energy band-likes and mean that in any fixed field region of a Hall plateau the electron-pairs occupy the same energy band-like.

It should be indicated that for a fixed magnetic field $B_{n|m}^{(l)}$ there exist two sets of the solutions $(\psi_{nm}^{(l)}, E_{nm}^{(l)})$ for $m = \pm|m|$, which work with a certain probability respectively. In Eq. (13) we only take into account of the diamagnetic states $\psi_{n,-|m}^{(l)}$ with lower energy $E_{n,-|m}^{(l)}$. Under some perturbations, the paramagnetic states with $m = |m| \neq 0$ may play an important role.

3. Quantum Hall plateaus and their widths

We now try to apply the above-mentioned results to a 2D electronic gas by using the electron-pair picture compared to the one-electron picture [5]. Because of the $(M_{nc} + 1)$ degenerate states of the center-of-mass motion and the non-degeneracy of the relative motion, the different electron-pairs of the same energy are in the same relative state and different center-of-mass states for any fixed magnetic field B . There may be $2(M_0 + 1)$ electron-pairs to occupy the lowest Landau level of the center-of-mass motion with $n_c = 0$ and two of them labelled by (m_c, m) and $(m_c, -m)$ have the same mean radius $\bar{R}_{0m_c} = \sqrt{|m_c| + 1} a_c$, where $a_c = \sqrt{\hbar/(2m_{eff}\omega_{n|m}^{(l)})}$ is a constant for the given magnetic field. Running $|m_c|$ from 0 to M_0 gives $(M_0 + 1)$ different mean radius of the $2(M_0 + 1)$

electron-pairs. The multiple electron-pairs in the lowest Landau level seem to behave like the condensed Bosons. In last section, we have assumed that the quantized magnetic field values $\{B_{n|m}^{(l)}\}$ correspond to the center sites of the quantum Hall plateaus and energy band-likes. Therefore, we expect that the minima of the diagonal-resistivity appear at these sites. This expectation can be proved by the experimental data [1–3, 5] on the integral and fractional QHEs as follows. In order to compare the theoretical results with the experimental data, we rewrite the truncation condition as

$$B_{n|m}^{(l)} = B_0/(k\nu_{n|m}^{(l)}), \quad \nu_{n|m}^{(l)} = (\sigma_{n|m}^{(l)})^2/k, \quad (14)$$

where $\nu_{n|m}^{(l)}$ is defined as the theoretical filling factor by comparison with the experimental one ν in references [1–3, 5], parameter k is related to the sample properties and electronic densities, and can be determined by a single set of experimental data. For example, if we take $m_{eff} = 0.067m_e$, $\epsilon \approx 13$, then Eq. (10) gives $B_0 \approx 25$ T. The recent experimental value of magnetic field at $\nu = 1/3$ is $B|_{\nu=1/3} \approx 12.5$ T for the sample of modulation-doped GaAs/AlGaAs quantum well [3]. Thus Eq. (14) implies $k = B_0/(\nu B)|_{\nu=1/3} = 6$. However, it was observed that for different samples the $B|_{\nu=1/3}$ has different values [2]. In Tsui's experiment [1], this value reads $B|_{\nu=1/3} \approx 15$ T which is the largest magnetic field value corresponding to a Hall plateau. Therefore, there some different parameter sets such as $m_{eff} = 0.067m_e$, $\epsilon \approx 11.9$ and $\epsilon \approx 13$, $m_{eff} = 0.073m_e$ to fit the parameters $B_{1,0}^{(l)} = 15$ T, $B_0 = 2B_{1,0}^{(l)} \approx k\nu_{1,0}^{(l)}B_{1,0}^{(l)} = 30$ T and $k = 2/\nu_{1,0}^{(l)} = 6$.

Comparing the theoretical filling factor $\nu_{n|m}^{(l)} = (\sigma_{n|m}^{(l)})^2/6$ with the experimental one ν , good agreement is found in the experimental accuracy, as in Table 1. It is worth noting that the largest magnetic field $B_{1,0}^{(l)}$ of a Hall plateau has been scaled to fit the filling factor $\nu_{1,0}^{(l)} = 1/3$ here, which is a good approximation to the case of reference [1]. Experimentally, for a lower temperature the largest magnetic field corresponds to a smaller filling factor [2, 3], and the current experiments cannot determine its limit at zero temperature. In addition, differing from the previous theoretical results, $\nu_{n|m}^{(l)} = (\sigma_{n|m}^{(l)})^2/6$ determined by Eq. (9) may be some irrational numbers for $n \geq 3$. On the other hand, we can rewrite the relative energy of Eq. (10) as $E_{nm}^{(l)} = (n + m + |m| + 1)\hbar\omega_0/(6\nu_{n|m}^{(l)})$. For a fixed magnetic field, the energies of the diamagnetic states with $m < 0$ are lower than that of the paramagnetic states with $m > 0$. In units of $\hbar\omega_0$ the energy values of the diamagnetic states are given in the final line of Table 1.

In Table 1 we show the complete agreement between the experimental ν and theoretical $\nu_{n|m}^{(l)}$ for the experimentally wide Hall plateaus with $(\nu = 1/3, 1, 5/3, 2, 7/3, 3)$

Table 1. Comparison between the theoretical and experimental filling factors

ν	3	$\frac{7}{3}$	2	$\frac{5}{3}$	$\frac{4}{3}$	1	$\frac{69}{71}$	$\frac{13}{15}$	$\frac{4}{5}$	$\frac{2}{3}$	$\frac{2}{5}$	$\frac{1}{3}$
$\binom{l}{n m}$	(1) 1,4	(1) 1,3	(1) 2,0	(1) 1,2	(1) 19,0	(1) 1,1	(1) 11,0	(1) 9,0	(1) 7,0	(1) 5,0	(1) 3,0	(1) 1,0
$\nu_{n m}^{(l)}$	3	$\frac{7}{3}$	2	$\frac{5}{3}$	1.3788	1	0.9712	0.8601	0.7436	0.6198	0.4853	$\frac{1}{3}$
$E_{n,- m }^{(l)}$	0.1111	0.1429	0.2500	0.2000	2.4176	0.3333	2.0593	1.4335	1.7931	1.6134	1.3736	1

and the approximate agreement of 10^{-2} order for the experimentally narrow plateaus [1, 2]. Thus as a single phenomenon the integral and fractional QHEs are described comprehensively. This is a quite natural result. The differences between our analytical results and the data of reference [2] may be caused partly by the fact that the largest magnetic field in reference [2] is not fitted by the filling factor $\nu = 1/3$. Such a difference could be decreased [39] by taking parameters $k = 30$ and $\nu_{1,2}^{(l)} = 1/3 \sim B = 20$ T [2], which is associated with the different sample and electronic density, and the largest magnetic field $\nu_{1,0}^{(l)} = 1/15 \sim B = 100$ T without experimental correspondence, where the error of Table 1 at site $\nu = 2/5$ is corrected as accurate value $\nu_{2,0}^{(l)} = 2/5$. Finite-temperature effect may be another reason producing the above differences. Many theoretical narrow plateaus do not appear in the experiments of references [1, 2], because of the finite-temperature in experiment and the zero temperature assumption in theory. In fact, a narrow plateau could appear only for the lower temperature $T \leq 1.65$ K, and as temperature was raised above 4.15 K, no any plateau existed in the previous experiments [1, 2]. Therefore, we neglect a lot of data concerning theoretical narrow plateaus in the table.

For a fixed magnetic field $B = B_{n,|m|}^{(l)}$ with fixed n , $|m|$ and l , from Eq. (10) we have the fixed frequency $\omega = \omega_{n,|m|}^{(l)}$. In units of $\hbar\omega_{n,|m|}^{(l)}$, the lowest relative energy reads $E_{n,-|m|}^{(l)} = n + 1$. For the sample and electronic density fitting $k = 6$, the experimentally lower minima [1, 2] appear in $n = 1, 2$ states with lower relative energies $E_{n,-|m|}^{(l)}$ as in Table 1. This implies that for two neighboring states with near B values the lower minima corresponds to the lower relative energy. For example, the two neighboring Hall states $\nu_{1,1}^{(1)} = 1$ and $\nu_{11,0}^{(1)} = 0.9712$ have near σ and ω values, but Table 1 gives their relative energies as $E_{1,-1}^{(1)} = 0.3333\hbar\omega_0$ and $E_{11,0}^{(1)} = 2.0593\hbar\omega_0$ respectively. The former is much less than the latter, so the $\nu = 1$ state is more stable compared to the $\nu = 69/71$ state, since the height of quantum level of the pairing states can be related to stability of the quantum system. Table 1 seems

to exist a counter example at $\nu = 5/3$, where the energy $E_{1,-2}^{(1)} = 0.2000$ is lower than the energy $E_{2,0}^{(1)} = 0.2500$ of the stable neighboring state at $\nu = 2$. This can be easily explained by taking into account of the paramagnetic state with energy $E_{1,2}^{(1)} = 0.3600$ for the same magnetic strength $B_{1,|2|}^{(1)} = B_{1,|-2|}^{(1)}$. If the states $\psi_{1,-2}^{(1)}$ and $\psi_{1,2}^{(1)}$ work with the same probability 0.5, the average relative energy reads $\bar{E} = 0.5(0.2000 + 0.3600) = 0.2800$ which is greater than the $E_{2,0}^{(1)}$.

Noticing that the total state and total energy have the forms $\Psi = \psi_{n_c m_c}^{(c)}(R)\psi_{nm}^{(l)}(r)$, $E_T = E_{n_c m_c}^{(c)} + E_{nm}^{(l)}$. In the case of fixed $B_{n,|m|}^{(l)}$, the lowest total energy reads $E_{0,-|m_c|}^{(c)} + E_{n,-|m|}^{(l)} = E_{0,0}^{(c)} + E_{n,-|m|}^{(l)}$, which corresponds to the $M_0 + 1$ lowest degenerate states $\psi_{0,m_c}^{(c)}(R)\psi_{n,-|m|}^{(l)}(r)$ for $m_c = 0, -1, -2, \dots, -M_0$. Because lower energy state possesses higher stability, we expect that for two neighboring Hall states of two different energies there are more electron-pairs in the lower degenerate states of the lower energy, which leads to lower minimal diagonal-resistance. The lower minimum of diagonal-resistance is associated with the wider Hall plateau in the experiments [1, 2]. Defining the width of $\nu_{n,|m|}^{(l)}$ plateau as $L_{n,|m|}^{(l)}$, we estimate the width ratio of two neighboring plateaus as $L_{n,|m|}^{(l)}/L_{n',|m'|}^{(l)} = \alpha E_{n',-|m'|}^{(l)}/E_{n,-|m|}^{(l)}$ with constant α to be determined by experimental conditions. This implies the width ratio $L_{1,1}^{(1)}/L_{11,0}^{(1)} = \alpha E_{11,0}^{(1)}/E_{1,-1}^{(1)} = 2.0593\alpha/0.3333 = 6.1779\alpha$. If we consider the paramagnetic state $\psi_{1,1}^{(1)}$ with the same weight, the average relative energy at $\nu = 1$ state reads $\bar{E} = 0.5000$ and the above width ratio becomes 4.1196α . The estimations of the diagonal-resistance minima and Hall plateau widths are in qualitative agreement with the existing experimental data [1, 2]. It is difficult to quantitatively calculate the plateau width and diagonal-resistance magnitude, since they depend on the sample temperature sensitively in the experiments [1, 2].

4. Conclusions and discussions

In conclusion, we have investigated the QHEs of a 2D electronic gas in a homogeneous magnetic field, based on the exact solutions of a magnetically trapped electron-pair which can be equivalent to a 2D hydrogen "pseudo-atom". The combined potential of the magnetic field and Coulomb field governs quantum motion of the electron-pair and results in the stable band-like structure consisting of the degenerate Landau levels of center-of-mass motion and the non-degenerate energy band-likes of relative motion. Some interesting and important physical properties are shown by using the exact and perturbed solutions and the band-like structure. Applying the results to explain the integral and fractional QHEs of a 2D electronic gas, we obtain the sites and strengths of the minimal diagonal-resistances, which are associated with the positions and widths of quantum Hall plateaus. The results are in good agreements with the well-known experimental data. Differing from the previous famous theory based on many-body wave functions [8, 9], our method based on the electron-pair states demonstrates a direct and simple connection between the band-like structure and the quantum Hall plateaus.

It is well known that the transport process of electrons is related to the diagonal-resistance ρ_{xx} , or equivalently, the direct conductivity σ_{xx} . At a wider Hall plateau the diagonal-resistance and direct conductivity vanish if there is no scattering process irrespective of the intensity of the field. The scattering process, e.g. by the impurities in a sample and between electrons, can lead to the nonzero diagonal-resistance. In our electron-pair picture, we have not taken into account of the effects such as the electron-scattering, impurities, finite-temperature, disorder, edge effects, electronic spins and the consequent spin Zeeman splitting. These effects may lead to more fine band-like structure to fit experimentally narrow plateaus better. Some of these effects can be treated as an effective correction to the exact electron-pair picture. Thus the exact pair states could play a similar role with the exact solutions of a hydrogen atom in the atomic shell structure theory. Although the electron-pair picture cannot quantitatively explain the fine quantum Hall structures, it is very important for understanding the integral and fractional QHEs comprehensively.

Acknowledgments

This work was supported by the National Natural Science Foundation of China under Grant Nos. 10875039 and 11175064, the Construct Program of the National

Key Discipline of China, the PCSIRT under Grant No. IRT0964 the SRFDPHE under Grant No. 200805420002, and the Hunan Provincial NSF(11JJ7001).

References

- [1] D. C. Tsui, H. L. Stormer, A. C. Gossard, *Phys. Rev. Lett.* 48, 1559 (1982)
- [2] H. L. Stormer, A. Chang, D. C. Tsui, J. C. M. Hwang, A. C. Gossard, W. Wiegmann, *Phys. Rev. Lett.* 50, 1953 (1983)
- [3] W. Pan, H. L. Stormer, D. C. Tsui, L. N. Pfeiffer, K. W. Baldwin, K. W. West, *Phys. Rev. Lett.* 90, 016801 (2003)
- [4] K. von Klitzing, G. Dorda, M. Pepper, *Phys. Rev. Lett.* 45, 494 (1980)
- [5] K. von Klitzing, *Rev. Mod. Phys.* 58, 519 (1986)
- [6] T. Chakraborty, *Adv. Phys.* 49, 959 (2000)
- [7] A. Hansen, J. Kertész, *Philos. Mag. B* 77, 1301 (1998)
- [8] R. B. Laughlin, *Phys. Rev. Lett.* 50, 1395 (1983)
- [9] R. B. Laughlin, *Phys. Rev. B* 23, R5632 (1981)
- [10] F. D. M. Haldane, *Phys. Rev. Lett.* 51, 605 (1983)
- [11] B. I. Halperin, *Phys. Rev. Lett.* 52, 1583 (1984)
- [12] R. G. Clark, J. R. Mallet, S. R. Haynes, J. J. Harris, C. T. Foxon, *Phys. Rev. Lett.* 60, 1747 (1988)
- [13] J. R. Simmons, H-P. Wei, L. W. Engel, D. C. Tsui, M. Shayegan, *Phys. Rev. Lett.* 63, 1731 (1989)
- [14] R. E. Prange, S. Girvin, *The Quantum Hall Effect*, 2nd edition (Springer Verlag, New York, 1990)
- [15] J. K. Jain, *Phys. Rev. Lett.* 63, 199 (1989)
- [16] J. K. Jain, *Phys. Rev. B* 41, 7653 (1990)
- [17] S. C. Zhang, T. H. Hansson, S. Kivelson, *Phys. Rev. Lett.* 62, 82 (1989)
- [18] S. C. Zhang, T. H. Hansson, S. Kivelson, *Phys. Rev. Lett.* 62, 980 (1989)
- [19] D. H. Lee, S. C. Zhang, *Phys. Rev. Lett.* 66, 1220 (1991)
- [20] J. P. Eisenstein, H. L. Stormer, *Science* 248, 1510 (1990)
- [21] C. C. Chang, J. K. Jain, *Phys. Rev. Lett.* 92, 196806 (2004)
- [22] A. Fukuda et al., *Physica E* 40, 1261 (2008)
- [23] S. Fujita, Y. Tamura, A. Suzuki, *Mod. Phys. Lett. B* 15, 817 (2001)
- [24] W. Pan, H. L. Stormer, D. C. Tsui, L. N. Pfeiffer, K. W. Baldwin, K. W. West, *Int. J. Mod. Phys. B* 16, 2940 (2002)
- [25] M. A. Hidalgo, R. Cangas, *Physica E* 42, 1329 (2010)
- [26] M. Taut, *Phys. Rev. A* 48, 3561 (1993)
- [27] M. Taut, *J. Phys. A-Match. Gen.* 27, 1045 (1994)
- [28] M. Taut, *J. Phys. A-Match. Gen.* 28, 2081 (1995)

- [29] R. Pino, V. M. Villalba, *Phys. Status Solidi B* 211, 641 (1999)
- [30] W. Hai et al., *Int. J. Theor. Phys.* 39, 1405 (2000)
- [31] M. Alberg, L. Willets, *Phys. Lett. A* 286, 7 (2001)
- [32] M. Ahmad, H. Zaman, N. Rehman, *Cent. Eur. J. Phys.* 8, 422 (2010)
- [33] M. Ayub, H. Zaman, M. Ahmad, *Cent. Eur. J. Phys.* 8, 135 (2010)
- [34] J. M. Shi, F. M. Peeters, J. T. Devreese, *Phys. Rev. B* 48, 5202 (1993)
- [35] J. Zeng, *Quantum Mechanics* (Science Press, Beijing, 2000) (in Chinese)
- [36] L. Landau, *Z. Phys.* 64, 629 (1930)
- [37] C. Kittel, *Introduction to Solid State Physics*, 5th edition (John Wiley, New York, 1976)
- [38] P. W. Barmby et al., *J. Phys.-Condens. Mat.* 6, 7867 (1994)
- [39] W. Hai, [arXiv:cond-mat/0406771v2](https://arxiv.org/abs/cond-mat/0406771v2) [cond-mat.mes-hall]